HYBRID RENEWABLE ENERGY SYSTEMS FOR ISOLATED FARMS. A REVIEW
/
SISTEME HIBRIDE DE ENERGIE REGENERABILĂ PENTRU FERMELE INSULARIZATE. O TRECERE IN REVISTĂ

Maican E.*[1)], Vlădut V.[2)], Vîlcu C.[2)], Sorică C.[2)], Dorian M.[3)], Mirea D.P.[4)], Bogăţeanu R.[5)] [1]
[1)] "Politehnica"University of Bucharest, Faculty of Biotechnical Systems Engineering / Romania;
[2)]INMA Bucharest / Romania; [3)]ICPE-CA Bucharest / Romania; [4)]University of Bristol / UK; [5)]INCAS Bucharest / Romania
Tel: +40721090813; E-mail: constantin.vilcu@inma.ro
DOI: 10.35633/INMATEH-59-09

Keywords: *hybrid renewable energy systems, renewable power generation, environment protection, sustainable agriculture*

Abbreviations:

AC – Alternating Current;
CAE – Computer-Aided Engineering;
CAD – Computer-Aided Design;
CFD – Computational Fluid Dynamics;
DC – Direct Current;
HAWT – Horizontal-axis Wind Turbines;
HVAC – High Voltage Alternating Current;
HVDC – High Voltage Direct Current;
HK – Hydrokinetic;
HKS – Hydrokinetic System;
HRES – Hybrid Renewable Energy Systems;
MN – Micro-networks;
NPS – National Power System;
PLC – Programmable Logic Controller;
PV – Photovoltaic Panel;
RES – Renewable Energy Sources;
SPV – Solar Photovoltaic System;
VAWT – Vertical-axis Wind Turbines;
VRFB – Vanadium Flow Redox Battery;
WT – Wind Turbine;
WPS – Wind Power System;
WTS – Wind Turbine System.

ABSTRACT

In this paper a preliminary analysis of hybrid renewable energy systems (HRES) able to generate at least 100 kW electric power is carried out. Restrictions on the installed power of small farms that are in isolated locations and cannot connect to NPS generally diminish productive activities and, implicitly, profit. Depending on the renewable energy resources (sun, wind, hydro) the characteristics of the isolated location of the work point, the optimal HRES system required for an efficient operation of the agricultural farm even under isolated conditions can be determined by the synthesis elaborated in this paper.

Renewable energies that are characteristic to abiotic environment have been approached, describing the current technological methods of transforming them into electricity. Critical issues related to energy storage variants were also considered for periods of time when renewable sources are not sufficient to ensure the electricity consumption needs. The mathematical model of the process of generating electricity from renewable sources has been elaborated in order to perform the global energy calculation of the optimum hybrid system required for the isolated farm.

These elements lead to the determination of the technical-economic indicator ζ €/kW of the HRES system in the management of the agricultural farm from the perspective of a sustainable agriculture that produces more with lower costs and in environmentally friendly conditions.

REZUMAT

În prezenta lucrare se face o analiză preliminară a sistemelor hibride de energie regenerabilă (HRES) a căror putere electrică generată poate să acopere un necesar de min. 100 kW. Restricţiile privind puterea electrică instalată a fermelor agricole de mică anvergură care sunt amplasate în locaţii insularizate şi fără posibilitate de racordare la SEN diminuează în general activităţile productive şi implicit profitul. În funcţie de resursele de energie regenerabile (soare, vânt, hidro) caracteristice locaţiei terestre insularizate a punctului de lucru se poate determina prin sinteza elaborată în această lucrare sistemul optim HRES necesar unei funcţionări eficiente a fermei agricole chiar şi în condiţii izolate.

[1] *Maican E., Prof. Ph.D. Eng.; Vlăduţ V., Ph.D. Eng.; Vîlcu C., Ph.D. Stud.Eng.; Sorică C., Ph.D. Eng.; Dorian M., Ph.D. Eng.; Mirea D.P., Stud.; Bogăţeanu R., Ph.D. Eng.*

S-au abordat tipurile de energii regenerabile caracteristice mediului abiotic prin descrierea metodelor tehnologice actuale de transformare a formei lor in energie electrică. S-a avut în vedere şi problematica critică referitoare la variantele de stocare a energiei pentru perioadele de timp în care sursele regenerabile nu sunt suficiente pentru asigurarea necesarului de consum de energie electrică. Modelarea matematică a procesului de generare a energiei electrice din surse regenerabile s-a elaborat în vederea realizării unui calcul global energetic al sistemului hibrid optim necesar fermei insularizate.

Aceste elemente conduc la determinarea indicatorului tehnico-economic ζ €/kW al sistemului HRES în managementul fermei agricole din perspectiva unei agriculturi durabile care produce mai mult cu cheltuieli mai mici şi în condiţii prietenoase cu mediul înconjurător.

INTRODUCTION

Energy is conceptually defined as a state function of a physical or chemical process. It can be obtained from exhaustible resources (non-renewable energy) or from the Sun and other inexhaustible resources (renewable energy) through conversion technologies in various forms of energy transfer. Table 1 shows the renewable energy sources (RES), the current conversion technologies used and the energy transfer form of the application, (*ECA, 2018*).

Table 1

Renewable energy sources, technologies and applications (*ECA, 2018*)

Source	Solar	Wind	Water	Waves, tides	Geothermal	Biomass, waste
Technologies	Photovoltaics, Solar thermal	Wind turbines	Hydropower plant	Dams, tidal barrages	Geothermal, heat pumps	Biomass comb biogas plants, biofuels
Applications	Electricity, Heating and Cooling	Electricity	Electricity	Electricity	Electricity, Heating and Cooling	Electricity, Heating and Cooling, Transport
% actually used in UE	6.4 %	12.7 %	14.4 %	- - -	3.2 %	63.3 % = (4.7 + 6.7 + 7.7 + 44.2)

Global use of non-renewable energy (coal, oil, natural gas) also has unwanted effects such as greenhouse gas emissions that have fuelled global warming, acid rain, ecological disasters or environmental pollution. Through current clean energy conversion technologies, renewable energy resources are becoming increasingly valued. In this context, renewable energy is a cross-cutting priority relevant to many EU policy areas. The EU provides support for renewable energy under several funding programmes, like the European Regional Development Fund (ERDF), the European Agricultural Fund for Rural Development (EAFRD) as well as the Horizon 2020 and LIFE programmes.

In Romania, in the agricultural sector, farmers become more and more interested in renewable energy sources (*Brunswick, 2019*). Fortunately, there are several renewable or alternative energy options available. However, it is often hard to identify which of the technologies are best suited to a specific farm operation. Fig.1 illustrates the country's energy potential for the following renewable resources: a) sun; b) wind and c) rivers.

Currently, converting solar energy into electricity directly through photovoltaic panels is the easiest method used globally to obtain electricity in the form of direct current from solar radiation reaching the surface of the Earth. At the upper limit of the atmosphere, the radiated sunshine energy is 1367 W/m^2 and measured at ground level on a surface perpendicular to the direction of the rays, can generally reach 1000 W/m^2. Analyzing the map of solar radiation at ground level in Romania (Fig.1a), (*SolarGis, 2019)* agricultural farms located in the south part of the country, such as Oltenia, Baragan and Dobrogea, are benefiting the use of solar energy.

For the exploitation of the wind resource at the location of the isolated farm, it is of interest to know the variation of the wind speed up to a height of 50…150 m in relation to the land surface and statistically in time, throughout the entire calendar year. Because wind power is proportional to its cube velocity (*Ehrlich R., 2013*), for designing and manufacturing wind power conversion systems, it is recommended that farmers first consult their farm positioning on the map from a wind resource point of view. From the analysis of the wind map of Romania presented in Fig. 1b), (*AddEnergy, 2019*) three wind potential areas are distinguished for the following average wind speeds: ~ 8 m/s - mountain area; ~ 6 m/s - the second area with wind potential that can be used cost-effectively (Black Sea coast, Danube Delta and northern Dobrogea, areas where wind

energy exploitation is favoured by lower wind turbulence); 4…5 m/s - the third area with considerable potential, which is the Barlad Plateau. Also, favourable wind speeds are reported in other more restricted areas in the western part of the country.

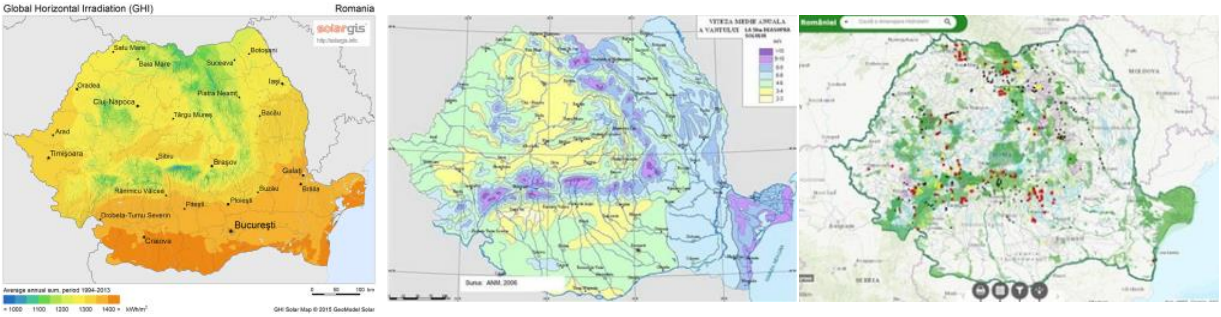

a) sun *b) wind* *c) rivers*

Fig. 1 – The country's energy potential for the renewable resources (RO)

The map of Romania's hydrographic network is presented in Fig.1c). Except rivers in the Dobrogea area, most of the running waters spring from the Carpathians and belong to the Danube river basin. Due to the varied configuration of Romania's terrain, the flowing water network is radially disposed. The main flowing waters have a longitudinal profile characterized by large slopes in the mountainous region where the water velocity is $v > 1$ m/s, while in the plain regions the water flow is more uniform, with lower velocities $v < 1$ m/s.

The most important RES in Romania is hydro energy (*WWF, 2019*). Agricultural farms located in the river meadows in the country's large river basins can benefit from the hydro-energetic micro-potential of fast rivers through simple facilities made to exploit the kinetic energy of flowing waters.

According to the RES maps in Fig.1, wherever it is located within the country, an isolated farm (without the possibility of connecting to the NPS) benefits from a dominant source of renewable energy. The other renewable resources are complementary so that a properly sized HRES system can continuously provide, through the integrated energy storage system, the power needed to operate in off-grid mode.

HRES is actually a combination of two or more renewable energy sources, or at least one renewable and one conventional source. HRES can be connected or not to the grid. For the presented case, the HRES system operates in stand-alone mode (off-grid mode). The hybrid energy system is defined as a combination of energy sources with different characteristics and an energy storage environment. With regard to stand-alone applications, choosing the optimal hybrid energy system is a challenging process due to many reasons, such as: determining the best combination of sources; reduce initial capital investment; reliability of power supply; system components, etc. Fig. 2 (*Zohuri B., 2018*) shows the block diagram of an autonomous hybrid system for small farms located in isolated locations. HRES hardware and software components are included in the Control System block and they perform process control and HRES efficiency improvement.

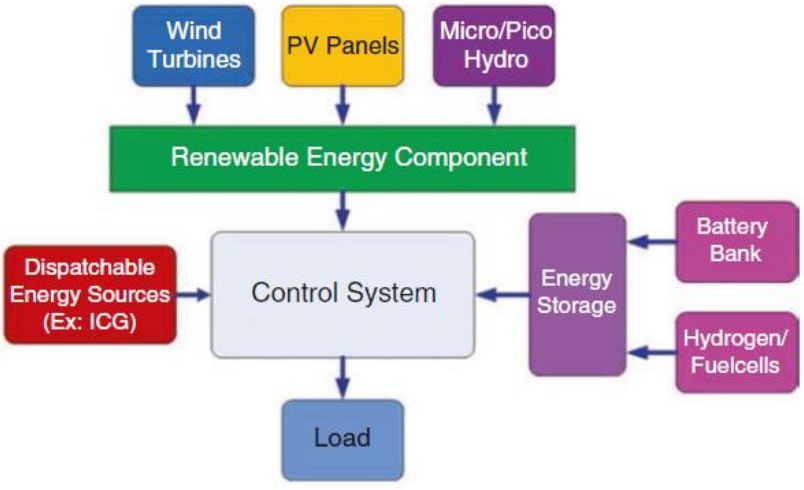

Fig. 2 – Diagram bloc of a stand-alone hybrid energy system
(*Zohuri B., 2018*)

The use in situ of HRES systems for isolated locations is a new step towards decentralized electrification. The systems can be grouped into single-phase or three-phase MNs, which feed local consumers and/or small farms. The interconnection of these sources of electricity in parallel on a common network raises many problems, caused mainly by their different functioning mode, by the different installed electric power, as well as by other particular aspects of each system. Often, in a HRES type system, in addition to renewable energy sources, conventional fossil fuel generators, generally Diesel engine generators, are used intermittently. They are introduced into the system when the demand for electricity of the consumers exceeds the capacity of the renewable sources. Combinations of more than two renewable sources become complex hybrid systems requiring higher-order investments. Reducing the techno-economic *ζ [€/kW]* indicator of such a hybrid energy system involves complex studies and detailed analyses before manufacturing. Fig. 4 shows the main systems of a hybrid HRES network: solar, wind, hydrokinetic, energy storage.

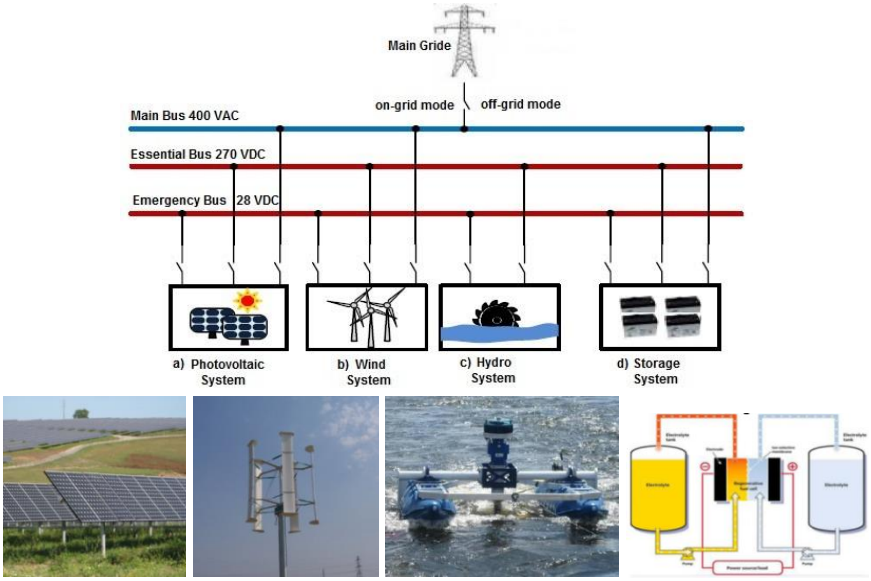

a) SPV b) WT c) HK d) VRB storage

Fig. 4 – Micro-grid topology of hybrid renewable energy systems

Source (MICROREN, 2015)

METHODOLOGICAL APPROACH TO THE HRES SYSTEM FOR SMALL FARMS

1. ESTABLISHED SYSTEMS FOR RENEWABLE ENERGY CONVERSION INTO ELECTRICAL ENERGY

1.1. Solar energy conversion system into electricity. PV technology and computational elements

Made out of semiconductor materials, the photovoltaic panels (PV) make direct conversion of solar energy into continuous current due to the photoelectric effect. Being the easiest method to convert solar radiation into electricity, PV technology is used today at any scale (Fig.5a). Typically, solar panels are modular, being made from sets of 36, 60 or 72 photovoltaic cells depending on the destination of the application in which they can be used. Voltage and PV power is directly proportional to the number of cells per module.

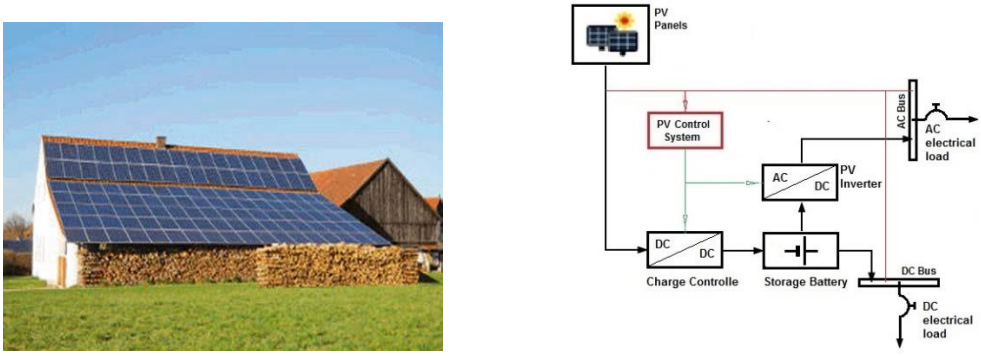

a) The isolated farm location (Zohuri B., 2018) *b) Block diagram of a SPV system*

Fig. 5 – Basic structure of a photovoltaic system (SPV)

Depending on the type of material from which the photovoltaic cells are made of (Si - silicon, GaAs - gallium arsenide, CdTe - cadmium telluride or based on polymers), their conversion efficiencies range between 8 % and 25 % in standard operating conditions (cell temperature: 25° C, irradiance of incident light perpendicular to the cell: 1000 W/m^2, air mass index: AM = 1.5), and can reach up to 44% for PVs with satellite-space destination. The efficiency of photovoltaic conversion decreases with the decrease of solar radiation. Photovoltaic cells are characterized by the current-voltage (IU) characteristic and by the power curve that leads to the determination of the nominal cell power, (*Maican E., 2015*). The basic block diagram of the SPV photovoltaic system corresponding to a small farm is shown in Fig.5b). A preliminary global calculation of electric power generated by the SPV system is based on the formula (*Bhandari et al., 2014*):

$$P_{SPV} = \eta_{PV} * G * A_t \quad [W] \tag{1}$$

where: G – represents the solar irradiation at the location of the farm: (0…1367) [W/m^2];

A_t – total area for n panels installed in the system with active surface A_{PV} given by the following relationship:

$$A_t = n * A_{PV} \quad [m^2] \tag{2}$$

η_{PV} – the conversion efficiency of solar energy into alternating current (AC) is given by:

$$\eta_{PV} = \eta_{DC} * \eta_{AC} * \eta_{GC} \tag{3}$$

where:

$\eta_{DC} \cong 0.25$ – efficiency of photovoltaic cells under standard operating conditions; (4)

$\eta_{AC} \cong 0.77$ – DC - AC conversion efficiency of the SPV system; (5)

$\eta_{GC} \cong 0.90$ – PV efficiency correlated with other global operating coefficients: dust and impurities, trajectory and PV position orientation, old panels, etc. (6)

For an average conversion efficiency ($\eta_{PV} \cong 17.325\ \%$) corresponding to the photovoltaic panels and the industrial electrical equipments integrated into the SPV system, from equation (1.1) one can obtain in 3D coordinates the variation of the electric power generated as a function of two variables:

$$P_{SPV} = f_1(G, A_t) = 0.17325 * G * A_t \quad [W] \tag{7}$$

For $G \in (0, 1400)$ W/m^2 and $A_t \in (100, 1000)$ m^2, the 3D-chart from Fig.6a) is plotted. As an example, for an average solar radiation of $G \cong 1230$ [W/m^2] from the farm location, the chart in the Cartesian coordinates from Fig.6b) is given by: $P_{SPV} = f_1(1230, A_t)$. From the preliminary analysis, depending on the load installed on the farm, the number of photovoltaic panels of the SPV system is calculated so that the necessary power is provided for a safe operation of the local consumers.

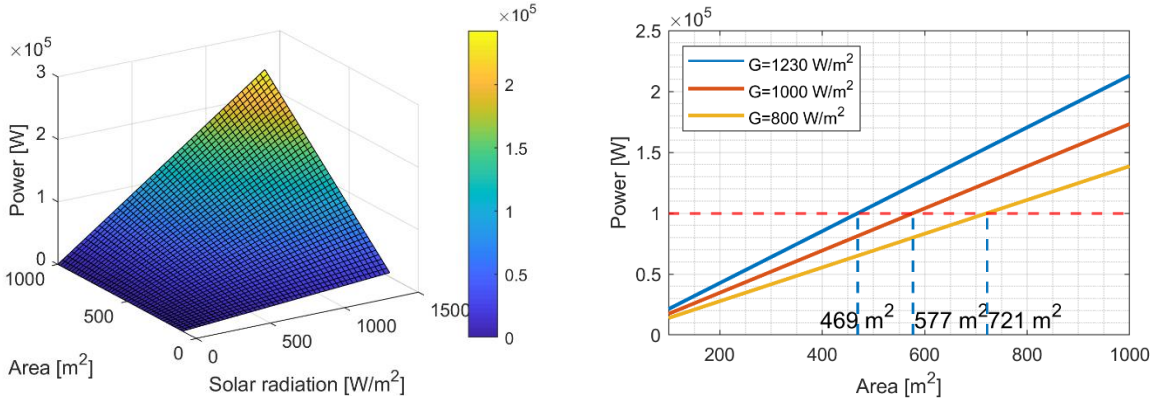

a) $P_{SPV} = f_1(G, A_t)$ b) $P_{SPV} = f_1(1230, A_t)$

Fig. 6 – The power variation chart generated by an SPV system depending on PV area and solar radiation

The single-wire electrical diagram in Fig.7 shows the configuration of the SPV solar system for stand-alone operation. The integrated hardware of the SPV system consists in the following devices: Battery Charge Controller, PV Inverter, PLC - DC power supply and SPV Control System. The command and control system of the SPV monitors the power generation process and, by means of the S1 ÷ S6 switches, controls the interconnection of the power distribution bars through the integrated devices. The software implemented in the SPV Control System increases the reliability of the solar power generation system and ensures the amount and quality of energy for both DC and AC consumers.

The connection diagram anticipates the possibility of further developing a hybrid system by setting up the electric circuits on an HVDC Essential Bus 270 VDC.

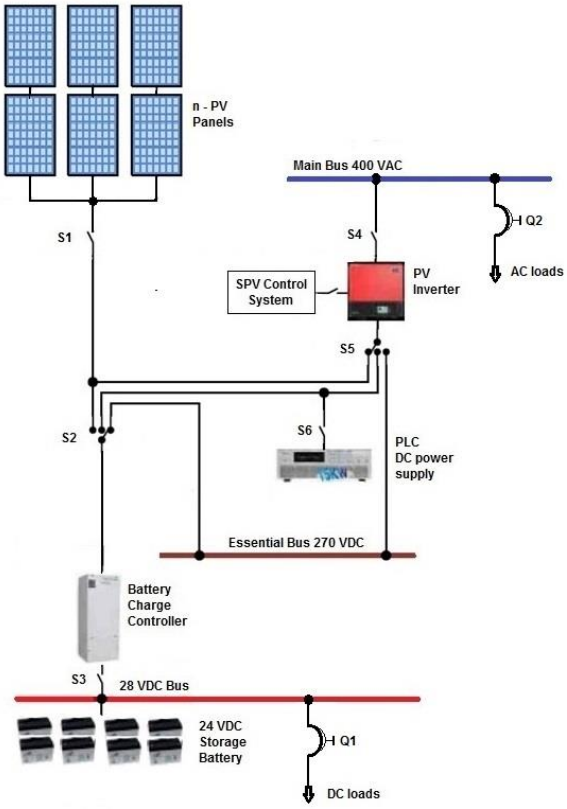

Fig. 7 – Schematic diagram on the SPV in off-grid mode (stand-alone)

1.2. *Wind power conversion system; Giromill technology and computational elements*

Wind energy is converted into electricity by wind turbines (WT). Currently, there are two basic categories of wind turbines: horizontal axis (HAWT) and vertical axis wind turbines (VAWT), depending on the orientation of the rotor axis. A wind turbine consists of three basic components: the rotor, gearbox or multipurpose drive and power generator. The rotor is a fluid-dynamic machine that converts the kinetic energy of an airflow into mechanical energy. The multiplier connects the turbine rotor to the electric generator with the transmission ratio required for the gearbox. The electric generator (asynchronous or synchronous) converts mechanical energy into electricity and delivers it to an electrical network, directly or via a transformer to the installed load.

Regardless of the WT type, depending on the rated electric power of the generator in the grid, wind turbine systems (WTS) are divided into three categories: small, for $P_{WTS} \leq 100\ \mathrm{kW}$; average, for $100\ [\mathrm{kW}] < P_{WTS} < 1\ \mathrm{MW}$; large, for $P_{WTS} \geq 1\ \mathrm{MW}$. The Danish HAWT turbines, also considered classic WT, dominate the global energy market for large category WTS.

Giromill type VAWT turbines (Fig.8b) are H-Darrieus turbines frequently used in agricultural applications for which the installed power load is lower than 100 kW. Figure 8a shows the efficiency of WT rotors for various types of wind turbine models. The theoretical wind turbine power coefficient C_p cannot exceed the limit of $\frac{16}{27}$, as calculated by Albert Betz based on the principles of energy conservation (*Patel M.R., 2006*). Various approaches, with a variety of weightings of the involved parameters, have been published. In the case of H-Darrieus wind turbines, most authors specify values of 0.32 to 0.42 for the maximum C_p (*D'Ambrosio M., 2010*). Wind power is described by the following equation:

$$P_w = \frac{1}{2} \cdot \dot{m} \cdot v^2 = \rho \cdot R \cdot h \cdot U^3 \quad [\mathrm{W}] \tag{8}$$

where:

$\dot{m}$ – air mass flow, given by: $\dot{m} = \rho \cdot A \cdot v$ [kg/s];

ρ – air density [kg/m^3];

A – area of the rotor surface [m^2]; for Giromill: $A = 2R \cdot h$;

R – rotor radius [m];

h – height of the rotor blades [m];

v – wind speed (U) [m/s].

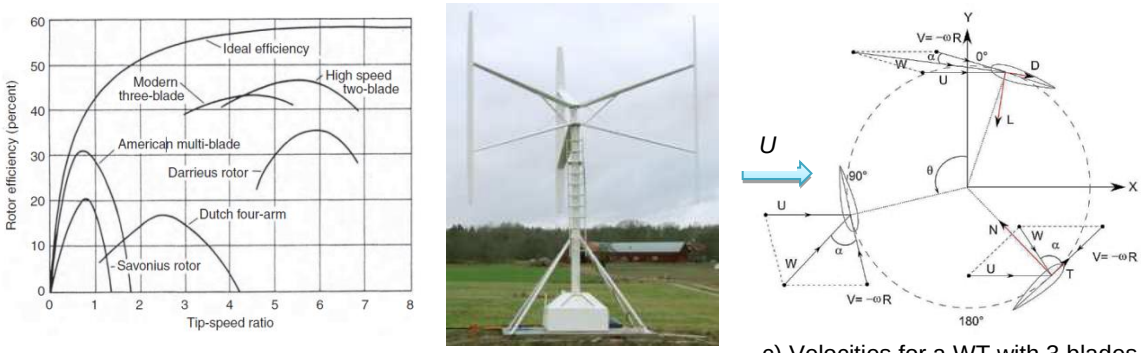

a) C_p=f(λ) b) Giromill WT (20 [kW]) c) Velocities for a WT with 3 blades

Fig. 8 – Basic data on the wind turbines system (WTS)

a) Rotor efficiency vs. TSR (tip-speed ratio) for different types of WT; b) Giromill WTS; c) The fluid-dynamic kinematics of a Giromill wind turbine

As an example, Fig. 8b shows the size of a 3-bladed Giromill WT with a nominal power of 20 kW, (*D'Ambrosio M., 2010*). Using Eq.8 for a turbine in this category and taking into account the rotor efficiency, the mechanical power obtained at the WT axis is given by (*Malael I., 2019*):

$$P_m = C_p \cdot \left(\frac{1}{2} \cdot \rho \cdot A \cdot v^3\right) = C_p \cdot \rho \cdot R \cdot h \cdot U^3 \quad [\text{W}] \tag{9}$$

Cp depends on wind speed, turbine speed, aerodynamic solution of WT and aerodynamic profile chosen for the blade. The TSR (tip-speed ratio) is defined as:

$$\lambda = \frac{\omega \cdot R}{U} \tag{10}$$

where the meanings of U, R, ω are shown in Fig. 8c).

Wind power *(P_w)* acts on the wind turbine blades and is converted into mechanical power to the turbine shaft *(P_m).* By means of a mechanical transmission with efficiency η_t, the power to operate the electric generator is $P_t = \eta_t \cdot P_m$. The electric power produced by the generator is $P_g = \eta_g \cdot P_t$, where η_g is the generator efficiency. If P_{WTS} is the electric power *(P_g)* produced by the wind system, one can calculate that:

$$P_{WTS} = C_p \cdot \eta_t \cdot \eta_g \cdot \left(\frac{1}{2} \cdot \rho \cdot A \cdot v^3\right) = \eta_{WTS} \cdot \frac{\rho A U^3}{2} \quad [\text{W}] \tag{11}$$

where: η_{WTS} – wind turbine system efficiency, whose value is maximized by increasing the performance coefficient of the turbine Cp. Equation 11 is based on the diagram of the WPS system presented in Fig. 9.

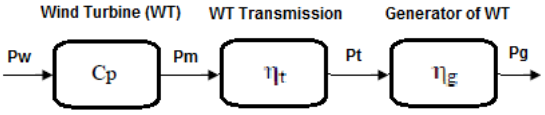

a) P_g – Power generated by the wind turbine

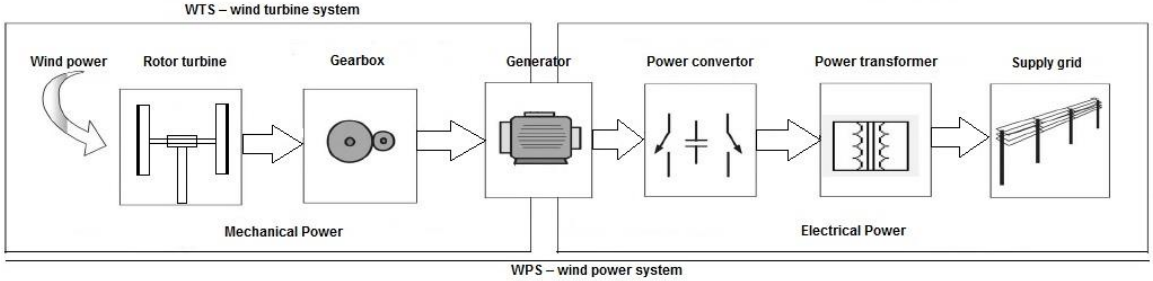

b) P_{WTS} – The electric power for the wind system injected in the grid (*Chen Z., Guerrero J.M, Blaabjerg F., 2009*)

Fig. 9 – Basic data on the power generated by the WPS, source (*MICROREN, 2015*)

Often, the preliminary calculation of the C_p performance coefficient is made by semi-empirical methods. The calculation method allows determining the power and torque of the vertical axis wind turbine

based on the load factor and forward resistance coefficients determined experimentally for the selected aerodynamic profile of the turbine blade.

According to Fig. 8c), the following parameters are defined:

U - upstream undisturbed wind speed; R - rotor radius WT;

V - the tangential speed of the turbine rotor blade; θ - the variation angle of the blades;

W - the resulting wind speed on the turbine blade; ω - angular velocity of the blade.

A discretization of the variation angle of the blades θ_i is chosen in the range of 0° to 360°. For each angle of variation $\theta_i \in$ (0°, 30°, 60°, 90°) the following algorithm is executed:

Step i). It is assumed, as a first approximation, that the velocity of the blade in position *i*, V_i, is equal to the upstream undisturbed wind speed, U:

$$a_i = \frac{V_i}{U} = 1 \tag{12}$$

where a is the speed loss coefficient.

Step ii). The incidence angle is calculated:

$$\alpha_i = arctan\left(\frac{V_i cos\theta_i}{\lambda U - V_i sin\theta_i}\right) + \alpha_0 \tag{13}$$

where α_0 is the angle of attack, and λ is the ratio of the peripheral velocity of the blade to the undisturbed airflow speed (2.3).

Step iii). Calculate the resulting speed:

$$W_i = \sqrt{(V_i cos\theta_i)^2 + (\lambda U - V_i sin\theta_i)^2} \tag{14}$$

Step iv). Calculate the Reynolds number:

$$Re_i = \frac{W_i b}{\nu} \tag{15}$$

where b is the length of the chord line, and ν is the kinematic viscosity of the air.

Step v). Calculate the coefficient of the normal force:

$$C_{n,i} = C_z(\alpha_i) cos\alpha_i + C_x(\alpha_i) sin\alpha_i \tag{16}$$

where C_x and C_z are the drag and load strength coefficients, respectively, determined experimentally in accordance to blade profile and angle of incidence.

Step vi). Calculate the function of the speed loss coefficient:

$$G(a) = \frac{Nb}{8\pi R|cos\theta_i|}\left(C_{n,i} cos\theta_i + C_{t,i} sin\theta_i\right)\frac{W_i^2}{V_i^2} \tag{17}$$

where N is the number of rotor blades and $G_a = G(a_i)$ for i-th iteration.

Step vii). The speed loss ratio is recalculated:

$$a = \frac{1}{1 + G_a} \tag{18}$$

The above steps are repeated until the desired precision is reached; the torque is determined for each θ_i:

$$T_i = \frac{\rho R W_i^2 b C_t h}{2} \tag{19}$$

where h is the height of the turbine.

Step viii). The torques generated by each blade are added for each angle of variation, and the turbine total torque is determined according to θ_i. The average torque (T_{med}) of the wind turbine is the average of these values, and the resulting average power is given by:

$$P_{med} = \omega \cdot T_{med} \tag{20}$$

Step ix). Finally, if the wind power is given by the Equation 8, then the wind turbine coefficient of performance is calculated as:

$$C_p = \frac{P_{med}}{P_w} = \frac{\omega \cdot T_{med}}{\rho R h U^3} \tag{21}$$

Although laborious, the calculation methodology presented can be simplified by means of CAE techniques. Figure 10 shows the CFD analysis of the hydrodynamic flow for a Giromill three-bladed rotor, using the ANSYS Fluent software package.

From the CFD numerical simulations performed on the rotor of a three-blade Giromill wind turbine, the performance coefficient $Cp \cong 0.37$ was determined to be optimal for the given application.

Taking into account that the efficiency of the mechanical transmission is $\eta_t \cong 0.98$ and for the integrated electric generator working in this power category is $\eta_g \cong 0.92$, the efficiency of the WTS system is:

$$\eta_{WTS} = C_p \cdot \eta_t \cdot \eta_g = 0.37 \cdot 0.98 \cdot 0.92 \cong 0.334 \quad (22)$$

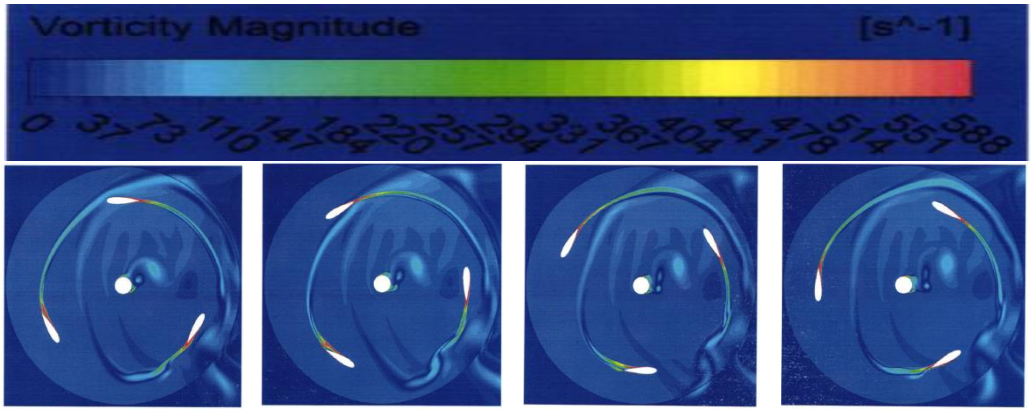

Vorticity Magnitude V = 11 [m/s] for TSR = 2

Fig. 10 – CFD analysis for a three-blade Giromill rotor

Substituting the determined value for η_{WTS} in Equation 11, the variation of the generated electric power as a function of two variables (A, U) is obtained:

$$P_{WTS} = f_2(A, U) = \frac{0.344}{2} \cdot \rho \cdot A \cdot U^3 \quad [\text{W}] \quad (23)$$

where: $\rho = 1.225$ kg/m³ is the air density for the location of the WT.

With the following predefined domains: $A \in (10, 100)$ m² and $U \in (0, 15)$ m/s, one can get the 3D chart in Fig. 11a). As an example, for a wind speed $U \cong 8$ [m/s] at farm location, and in order to generate an electric power of 30 kW, the required area of the H-type rotor of a Giromill wind turbine is determined from the plot in Fig. 11b). Similarly, the WTS analysis is performed for other wind speeds.

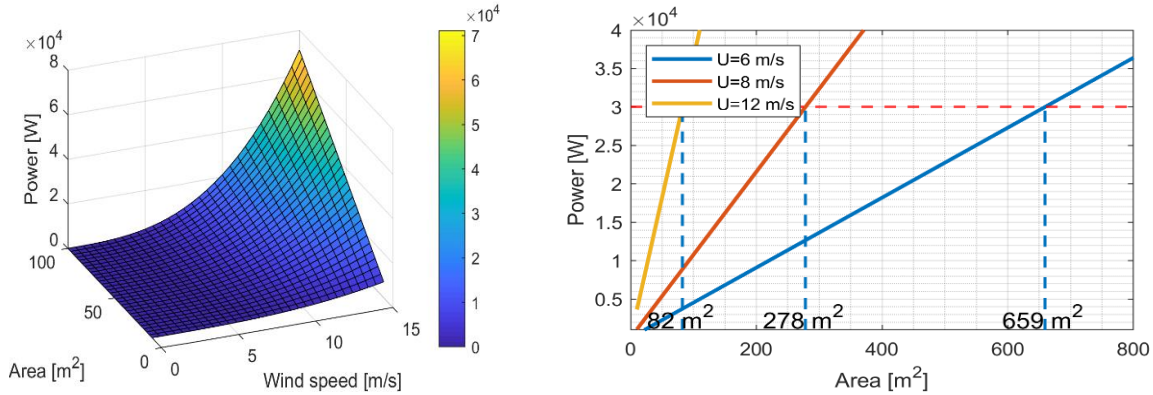

a) $P_{WTS} = f_2(A, U)$ b) $P_{WTS} = f_2(A, 6)$; $P_{WTS} = f_2(A, 8)$; $P_{WTS} = f_2(A, 12)$

Fig. 11 – Plots of the power variation generated by a WTS, depending on rotor area and wind speed

VAWT wind turbines have the advantages of no guidance systems and heavy equipment (gearbox, electric generator, etc.) located close to the ground. The main disadvantage of the classic solution is the vertical shaft provided with a top bearing that requires ground anchorage. This disadvantage is overcome by the Girromill solution (H-Darrieus) and makes VAWTs feasible especially for relatively small powers. The connections diagram from Fig. 12b) shows the configuration of the WTS for the autonomous mode (off-grid).

The hardware integrated into the WTS system consists of Wind Inverter, Wind Interface, WTS Control System, Hybrid Inverter and Battery Charge Controller. The WTS control system supervises the process of electricity generation and, by means of switches S2, S3, S7, … S9, controls the interconnection of the electricity distribution bars through integrated devices. The WTS Control System software increases the reliability of the wind power generation system and ensures the quantity and quality of energy for both DC

and AC consumers. The connection diagram also anticipates the possibility of developing a hybrid system of renewable energy by developing electrical circuits on a HVDC essential bus at 270V.

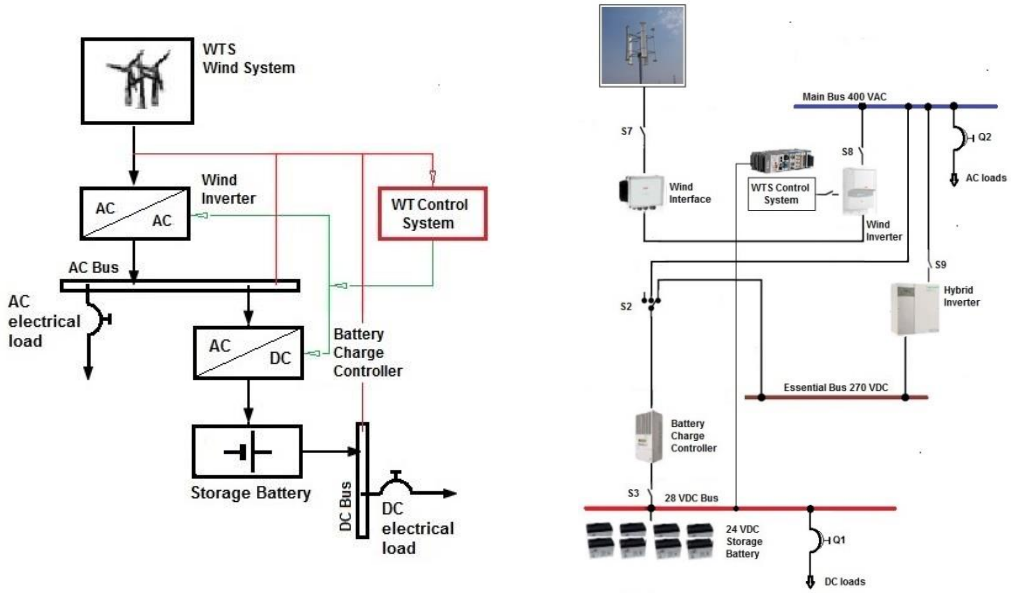

a) Block diagram of WTS *b) Sigle wire electrical connection scheme of WTS*

Fig. 12 –Schematic diagram of the WTS system for off-grid mode

1.3. Systems for hydropower energy conversion into electric power. Kaplan technology and computational elements

All systems converting the hydro energy into another form of useful energy exploit the potential energy of water (Fig. 13. *a*, *b*). The objective of a hydroelectric system is to convert the potential energy of the water flow (*Q*) flowing from a certain height (*H*) into electrical energy. The key element of the hydro energy conversion system is the hydraulic turbine (Fig. 13 *c*) which can be an impulse or a jet turbine. The mechanical torque is transmitted through a multiplier gear to an electric current generator, (*ENER-SUPPLY, 2012*).

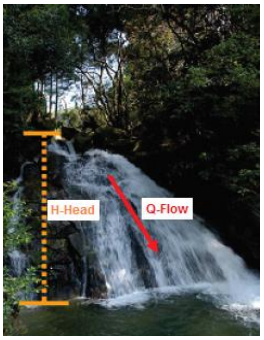

a) On-site hydro potential

b) In situ HKS installation

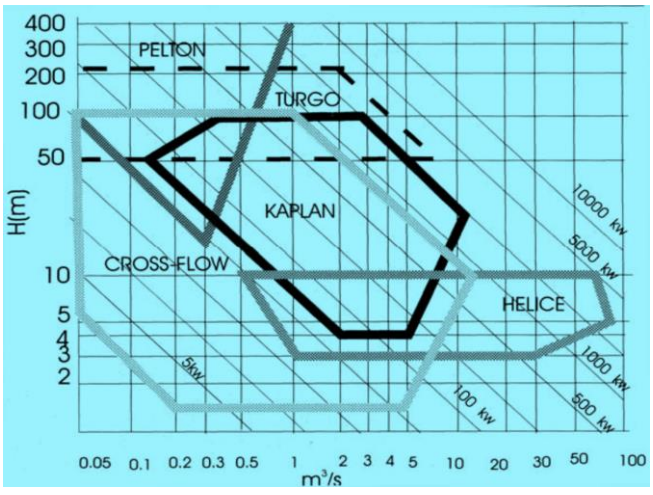

c) diagram of the applicability domains for hydro turbines

Fig. 13 – Basic data of the HKS system

The available power produced by the hydroelectric system is given by:

$$P_{HKS} = \eta_{HKS} \cdot \rho \cdot g \cdot Q \cdot H \quad [W] \tag{24}$$

where:

ρ – water density (1000 kg/m³); Q – water flow through the turbine [m³/s];
g – gravitational acceleration (9.81 m/s²); H – effective water drop at turbine level [m];
η_{HKS} – the efficiency of the hydroelectric system corresponding to the efficiencies of system components: hydraulic turbine, $\eta_{HT} \in (0.60 \div 0.80)\%$; mechanical transmission from the turbine to the generator, $\eta_t \cong 0.98$; integrated electric generator, $\eta_g \cong 0.92$; by substituting, the approximate value is:

$$\eta_{HKS} = \eta_{HT} \cdot \eta_t \cdot \eta_g = 0.80 \cdot 0.98 \cdot 0.92 \cong 0.727 \quad (25)$$

For a preliminary calculation, entering the value from (Eq.25) in (Eq.24), the power P_{HKS} can be written as:

$$P_{HKS} = f_3(Q,H) = 7.13 \cdot Q \cdot H \quad [\text{kW}] \quad (26)$$

Figure 14 shows the variation of $P_{HKS} = f_3(Q,H)$ in both 3D and Cartesian coordinates for preset values of *H*. For guidance, for unit values of $Q = 1$ m³/s and $H = 1$ m an electric power of $P_{SH} = 7.13$ kW is obtained. Multiplying this value with concrete values from the specific site gives the field of hydropower potential from the location of the isolated farm regarding the coverage of the required electric power. For the $Q \in (0, 10)$ m³/s and $H \in (0, 10)$ m, the 3D plot is shown in Fig. 14 *a*). For various water drops at turbine level ($H \cong 2;\ 4;\ 8$ m) from the farm location, the required water flow *Q* [m³/s] passing through the turbine to generate an electric power of 70 kW is automatically determined from the chart in Fig. 14 *b*).

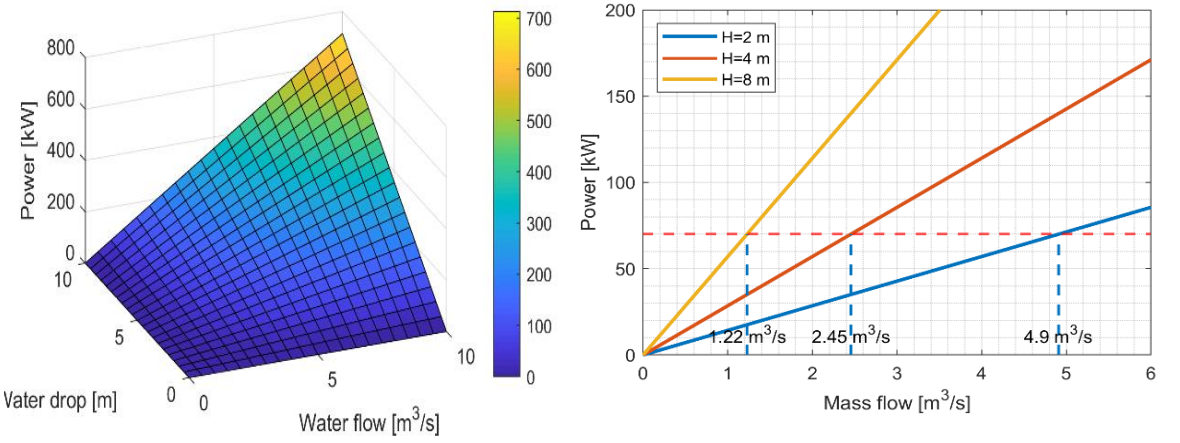

a) $P_{HKS} = f_3(Q,H)$ [kW]

b) $P_{HKS} = f_3(Q,2)$; $P_{HKS} = f_3(Q,4)$; $P_{HKS} = f_3(Q,8)$

Fig. 14 – The power variation graph generated by an HKS depending on Q and H

Low power hydroelectric stations include micro-hydroelectric power stations and hydro-kinetic systems (HKS) that can generate less than 100 kW electric power. HKS systems are anchored floating structures with the reactive turbine immersed, are installed on fast running surface water (see Fig. 13*b*), and does not require additional construction work. The water flow kinetic energy is converted directly into electrical energy through the system consisting of hydraulic turbine, multiplier gear, and synchronous generator.

For a floating hydro-kinetic system installed on the water surface, from Eq. 24, the produced power is determined by successive replacements, depending on the speed of the running water v_a and the active surface of the hydro turbine A_T:

$$P_{HKS} = f_4(A_T, v_a) = 363.6 \cdot A_T \cdot v_a^3 \quad [\text{W}] \quad (27)$$

where: ρ – water density (1000 kg/m³);
g – gravitational acceleration (9.81 m/s²);
R_e < 2000 – Reynolds number.

The 3D plot in Fig. 15 *a*) is obtained based on the following predefined values: $v_a \in (0, 5)$ m/s and $A_T \in (0, 5)$ m². For different water speeds at turbine level $v_a \cong 1;\ 2;\ 3$ [m/s] measured at farm location, the area of the turbine rotor surface A_T [m²] required to generate 10 kW is determined from Fig. 15 *b*). In Fig. 16

the block diagram of an autonomous hydro-kinetic system for isolated farm locations with the schematic representation of the local network is presented.

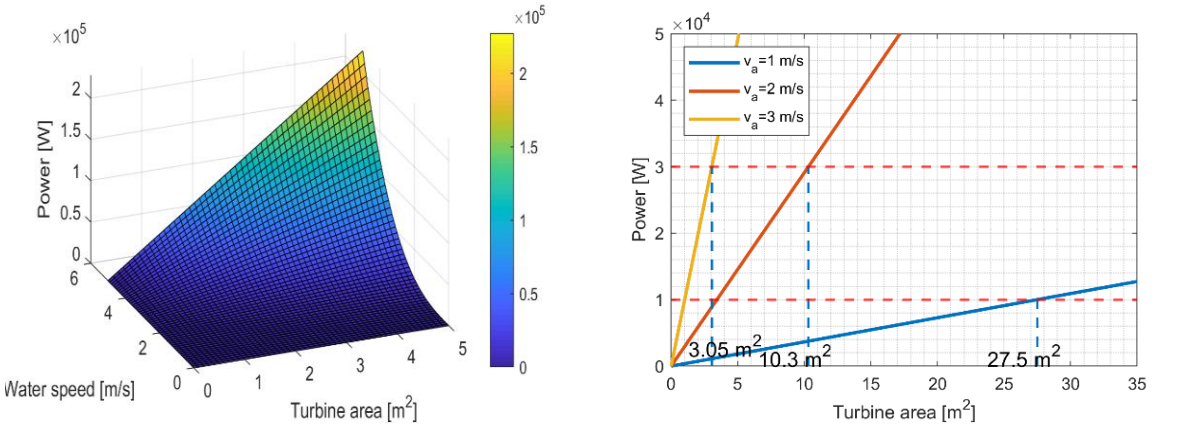

a) $P_{HKS} = f_4(A_T, v_a)$ b) $P_{HKS} = f_4(A_T, 1)$; $P_{HKS} = f_4(A_T, 2)$; $P_{HKS} = f_4(A_T, 3)$

Fig. 15 – Power variation graph generated by an HKS depending on turbine area and water speed

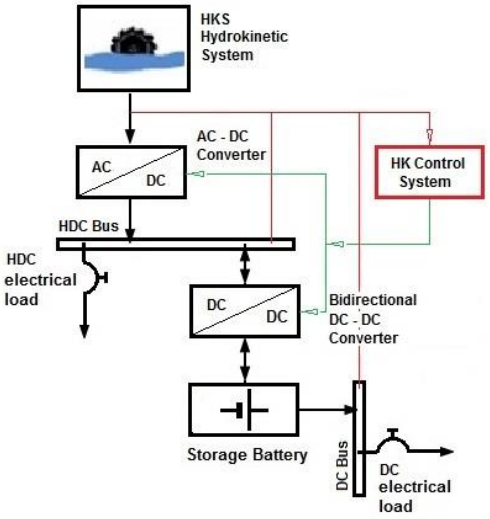

Fig. 16 – Schematic diagram of the HKS system in off-grid mode (stand-alone)

2. HYBRID CONVERSION SYSTEMS OF RENEWABLE ENERGY IN ELECTRIC POWER

2.1. Dual systems for converting renewable energy into electricity

Crucial for off-grid systems is the climate because it can make one type of hybrid system more profitable than another. Currently, the dual systems are most widespread in HRES applicability, being ideal no matter the location and climate of the area. The most frequently used are photovoltaic-wind systems. Fig. 17 presents the simplified connection diagram of a low-power HRES structure (the 230VAC / 50Hz single-phase hybrid micro-network at the University of Aalborg in Denmark, Institute of Energy Technology), (*E-FARM, 2008*). It consists of a Windy Boy 1.7 kW wind farm, a Sunny Boy 1.7 kW photovoltaic panels system, and a VRB energy storage system with redox-flow vanadium battery, interfaced with the microgrid through a Sunny Island 5048 inverter of 5 kW. The main micro-core component is the Sunny Island inverter that controls the microgrid (voltage and frequency) to provide optimal VRB battery usage. Depending on the required load and the power produced by the wind and photovoltaic systems, the Sunny Island inverter provides power balance, controlling the micro-grid frequency. The inverter can also provide the interconnection of the HRES micro-grid with the local public grid when the location allows it, (*E-FARM, 2008*). Thus, it becomes an Emergency system that automatically switches to off-grid mode when the University's main grid is faulty.

Other dual configurations are photovoltaic-hydro, wind-hydro, photovoltaic-geothermal, etc. All of them require the inclusion of an electrical energy storage system that can operate in a buffer with the generators connected in parallel through the interfacing equipment. In the case of dual stand-alone hybrid systems for increasing safety in operation, there is a third system, for emergency (fossil fuel powered generator set), which normally is in stand-by mode.

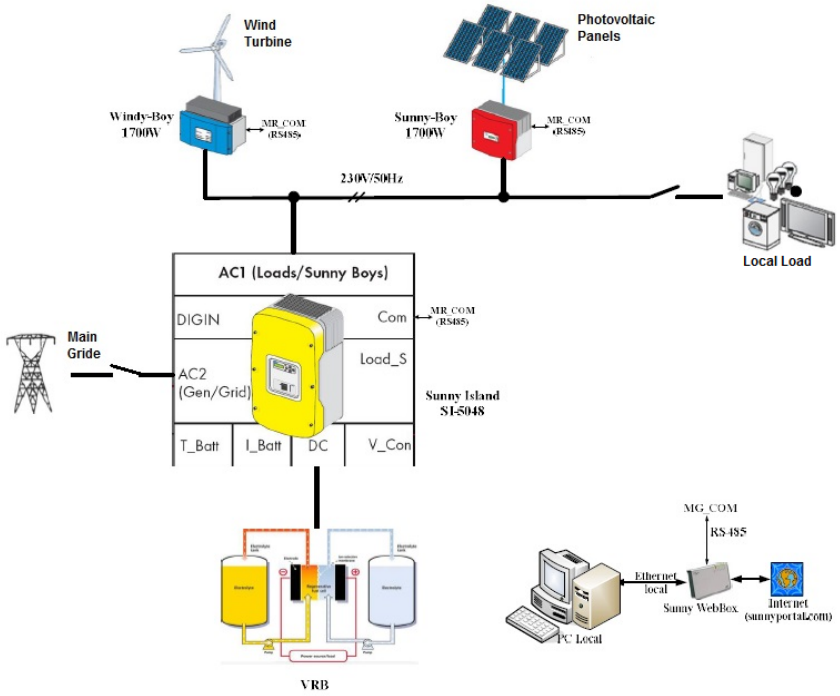

Fig. 17 – Micro-grid topology of HRES dual system (*E-FARM, 2008*)

2.2. A complex system to convert renewable energy into electricity for isolated areas

HRES are an adequate and competitive solution for rural electrification and/or for isolated agricultural farms. Reliability and cost are the two most important aspects that must be considered while designing the hybrid energy system. The most important advantage is that HRES makes best use of the renewable power generation technologies operating characteristics, and efficiency is higher than the one that could be obtained if a single power source is used (*Bajpai O., Dash V., 2012*). It can also address limitations in terms of fuel flexibility, efficiency, reliability, emissions and economics. A HRES network (Fig. 18) is composed of solar, wind, hydrokinetic and energy storage systems. In this research, the hybrid system is conceived as a complex HRES off-grid system for a payload of 100 kW, designed for isolated farms that cannot connect to NPS.

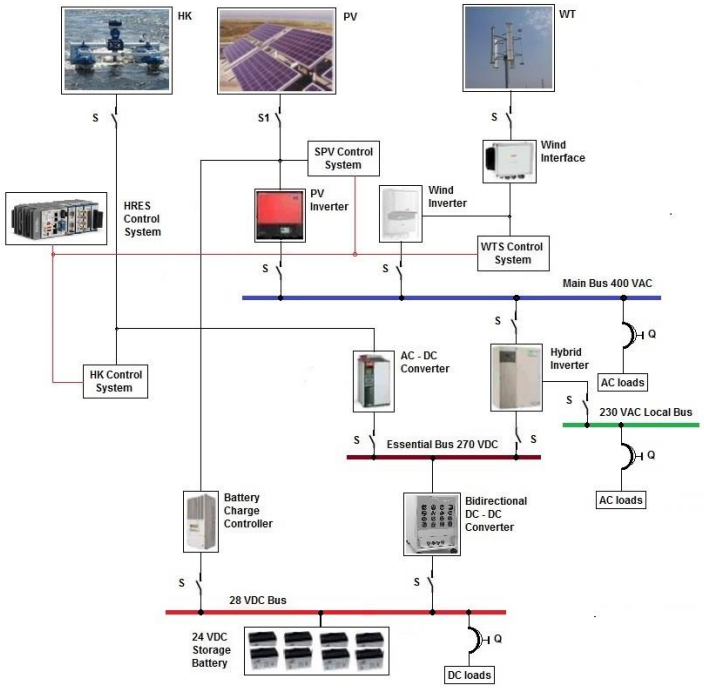

Fig. 18 – Block diagram of HRES stand-alone system for off-grid mode

The basic PV, WT and HK systems convert solar, wind and water hydro-kinetic energy into electrical energy respectively. This is injected into the bars of the energy node for electricity distribution, through the interfacing equipment of the micro-network. All electronic devices in Fig. 18 are installed in two separate cabinets, depending on the performed service. One cabinet includes electric elements and power circuits for conversion, switching and distribution of electricity through the protection elements. The second cabinet is for automation and includes elements and signal circuits with special purpose regarding the command and control of power generation, providing real time protection for the HRES micro-network. Due to the off-grid mode, the micro-network is designed on three levels that allow autonomous operation regardless of the external disturbances. The bars of the energy node have different voltages and are interconnected by the conversion elements, in order to operate in buffer with the energy storage system. Analogous to the energy systems on board the airplanes, the following configuration of the HRES micro-network is designed:

- Main Bus 400VAC, 50 Hz;
- Local Bus 230VAC, 50 Hz;
- Emergency Bus 28 VDC.
- Essential Bus 270 VDC

The reliability of the HRES system increases not only through the possibilities of interconnecting the voltage bars but also by integrating the System Controller, for real time process monitoring and for an optimum operation of the HRES hybrid system.

RESULTS AND DISCUSSIONS

For the small agricultural farm located in an isolated location (45°13'13.24" N; 28°45'24.75" E; elevation 7ft; Fig. 19 *a*), a total installed electric load of 100 kW was provided in order to carry out the farm activities under optimum working conditions. Local environmental data can be extracted from Fig. 19.

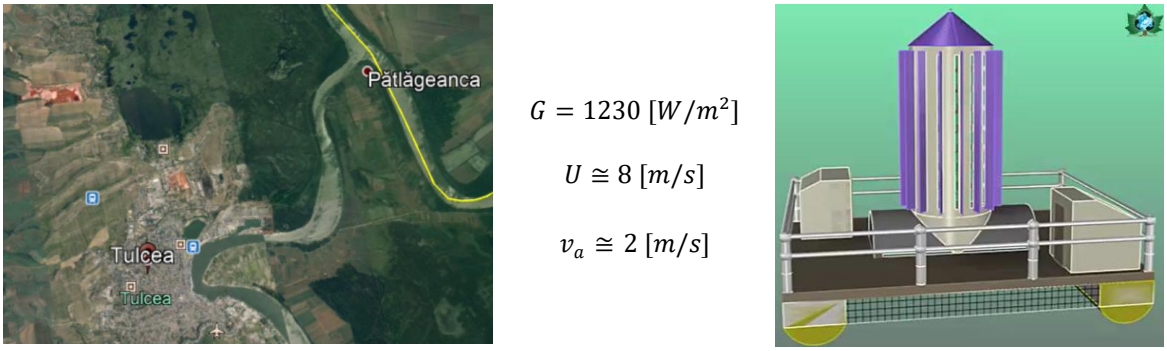

a) The farm location *b) Local environmental data* *c) TEACHERS HRES*

Fig. 19 – Location and primary environmental data for HRES

The hybrid HRES system is configured in the following order: photovoltaic, wind, hydrokinetic. HRES necessarily includes the electrical energy storage system consisting of battery packs and optionally an electro-generator group on fossil fuel, to be used as an emergency system. By means of the energy balance of the small farm simulated during one year of agricultural process, for an installed electric load of 100 kW an average power $P_m = 78.9$ kW is obtained. The HRES power generators are calculated to have the capacity to simultaneously inject into the energy distribution node an electric power of:

$$P^*_{HRES} = 1.10 * P_m = 86.79 \cong 87 \text{ kW} \quad (28)$$

Loads demands that give the short or long term peaks of electricity can be covered by the electricity storage system and/or by the emergency system.

The main component of HRES is the photovoltaic system (SPV). From Fig. 6 *b*), a total active panels' surface $A_t = 469$ m² corresponding to a maximum generated power $P_{SPV} = 100$ kW is chosen. Because the SPV system is characterized by the day-time power generation, a constraint was imposed: $P_{SPV} \geq P^*_{HRES}$ The second component of HRES is the WTS wind system. From Fig. 11 *b*), an active HAWT surface $A = 278$ m² corresponding to a maximum generated power $P_{WTS} = 30$ kW is selected. Because the WTS wind energy conversion system has a random characteristic of power generation, the following constraint was imposed: $P_{WTS} \leq \frac{1}{2} \cdot P^*_{HRES}$.

The tertiary component system of HRES is the HKS hydro-kinetic system. Considering Fig. 15 *b*), the chosen active surface of immersed turbines is $A = 10.3$ m², corresponding to a generated power of $P_{HKS} = 30$ kW. Because the HKS hydro power conversion system has size restrictions due to water depth, and because the running water speed is low, the following constraint is imposed: $P_{HKS} \leq \frac{1}{3} \cdot P^*_{HRES}$. HKS is the only HRES component system with continuous conversion of hydro-kinetic energy into electricity.

The electric power generated by the HRES hybrid system is the sum of the electric powers generated by each component:

$$P_{HRES} = \sum_{i=1}^{3} P_i = P_{SPV} + P_{WTS} + P_{HKS} \quad [\text{kW}] \tag{29}$$

Replacing the previously determined power values, the maximum power of the HRES system in the local micro-network of the farm is $P_{HRES} = 160$ kW. These peak operating moments are random, the surplus of electricity being taken over by the storage system.

The ratio between the maximum generated power and the calculated average one is:

$$\varsigma = \frac{P_{HRES}}{P^*_{HRES}} = 1.839 \tag{30}$$

This ratio represents the degree of over-dimensioning of HRES and it is necessary to provide the operational safety of the hybrid system. Fig. 19c presents a new concept of HRES system whose no. $\varsigma \rightarrow 1.0$

CONCLUSIONS

The aim of this article was to develop a calculation methodology for defining the component of a hybrid HRES system for converting renewable energy into electricity for a small farm in an isolated location. A preliminary global calculation was performed for a small farm in the Patlageanca cross-border area. The configuration of the hybrid HRES system is summarized in Table no. 2.

Table 2

160 k] HRES – Hybrid Renewable Energy Systems (sun, wind, water)				
# P.N.	System component	Basic data		
1.	The **SPV** photovoltaic system	$G = 1230$ W/m²	$A_t = 469\ m^2$	$\boldsymbol{P_{SPV} = 100}$ **kW**
2.	The **WTS** wind system	$U \cong 8$ m/s	$A = 278\ m^2$	$\boldsymbol{P_{WTS} = 30}$ **kW**
3.	The **HKS** hydro-kinetic system	$v_a \cong 2$ m/s	$A = 10.3\ m^2$	$\boldsymbol{P_{HKS} = 30}$ **kW**
4.	Electrical energy storage system	battery bank of 24V DC∗4000 Ah		
5.	Emergency system	It is optionally an electric-generator group on fossil fuel		
6.	The technical-economic execution indicator of the HRES system			$\boldsymbol{\zeta = 1.00}$ €/W
7.	The degree of over-dimensioning for operational safety of the HRES			$\boldsymbol{\varsigma = 1.839}$

ACKNOWLEDGEMENT

Within the project *"Innovative Technologies for Renewable Energy Production from Integrated Natural Sources in Complex Installations"*, which is carried out in contract 81PCCDI / 27.03.2018, through component no. 1 of the project *"Significant optimization of complex systems for the production of renewable energy in coastal and running waters"*, the documentation study on the stand-alone HRES hybrid systems was initially performed. This paper reviews the main RES systems and how they can be combined into a hybrid system. The optimal development of a complex hybrid system with applicability in the micro-networks of the isolated agricultural farms without possibility of connection to the NPS was followed.

REFERENCES

[1] Bajpai O., Dash V., (2012), Hybrid renewable energy systems for power generation in standalone applications: a review*, Renewable and Sustainable Energy Reviews*, vol. 16(5), pp. 2926-2939;

[2] Bhandari B., Poudel S.R., Lee K.T., Ahn S.H., (2014), Mathematical Modeling of Hybrid Renewable Energy System: A Review on Small Hydro-Solar-Wind Power Generation, *International Journal of Precision Engineering and Manufacturing-Green Technology*, vol. 1(2), pp. 157-173, Springer;

[3] Chen Z., Guerrero J.M., Blaabjerg F., (2009), A Review of the State of the Art of Power Electronics for Wind Turbines, *IEEE Transactions on Power Electronics,* vol. 24(8), pp. 1859-1875;

[4] D'Ambrosio M., Medaglia M., (2010), Vertical Axis Wind Turbines: History, Technology and Applications, Master Thesis in Energy Engineering, Halmstad University, Sweden;

[5] Ehrlich R., (2013), *Renewable energy, A First Course*, CRC Press Taylor & Francis Group, ISBN 978-1-4665-9944-4;
[6] Maican E., (2015), *Renewable energy systems*, (*Sisteme de energii regenerabile*), Printech Publishing House, Bucharest / Romania;
[7] Malael I., (2019), *TECC Project*; Retrieved from "COMOTI - Romanian Research & Development Institute for Gas Turbines": http://www.comoti.ro/ro/Proiect_TECC.htm?pag=3;
[8] Patel Mukund R., (2006), *Wind and Solar Power Systems: Design, Analysis, and Operation,* CRC Press Taylor & Francis Group, ISBN 9780849315701;
[9] SolarGis, (2019), *Solar resource maps of Romania*. Retrieved from "Weather data and software for solar power investments": https://solargis.com/maps-and-gis-data/download/omania;
[10] Zohuri B., (2018), Hybrid Renewable Energy Systems, Springer International Publishing AG 2018, https://doi.org/10.1007/978-3-319-70721-1_1, University of New Mexico, USA.
[11] ***AddEnergy, (2019), *Romania's Wind Energy Potential (RO: Potentialul eolian al Romaniei),* Retrieved from Add Energy Renewable: http://add-energy.ro/potentialul-eolian-al-Romaniei;
[12] ***Brunswick, (2019), An Introduction to Renewable Energy - Options for Farmers, https://www2.gnb.ca/content/dam/gnb/Departments/10/pdf/Agriculture/RenewableEnergy.pdf, Canada;
[13] ***ECA, (2018), Special Report no. 5, *Renewable energy for sustainable rural development: significant potential synergies, but mostly unrealised*, ECA – European Court of Auditors, 12, rue Alcide De Gasperi, 1615 Luxembourg;
[14] ***Ener-Supply, (2012), *Manual-Renewable Energy Sources*, (*Manual - Surse regenerabile de energie*), SEE Project, Energy Efficiency and Renewable Energies - Local Energy Support Policies;
[15] ***MICROREN, (2015), *Hybrid renewable energy conversion systems of small power integrated into a micro-network – MICROREN*, (Sisteme hibride de conversie a energiei regenerabile de mică putere integrate într-o microreţea – MICROREN), Scientific and technical report, PCCA project no. 36/2012 - stage 4 – 2015, Polytechnic University of Timisoara / Romania;
[16] ***WWF, (2019). *Romanian Rivers and the Impact of Hydro Energy Adjustments*. Retrieved from "Rivers of Romania": https://raurileromaniei.ro/harta/.